



Microstructural examination of carbonated 3D printed concrete

Journal Article

Author(s):

Aguilar Sanchez, Asel Maria; [Wangler, Timothy](#) ; Stefanoni, Matteo; [Angst, Ueli](#) 

Publication date:

2022-05

Permanent link:

<https://doi.org/10.3929/ethz-b-000532894>

Rights / license:

[Creative Commons Attribution 4.0 International](#)

Originally published in:

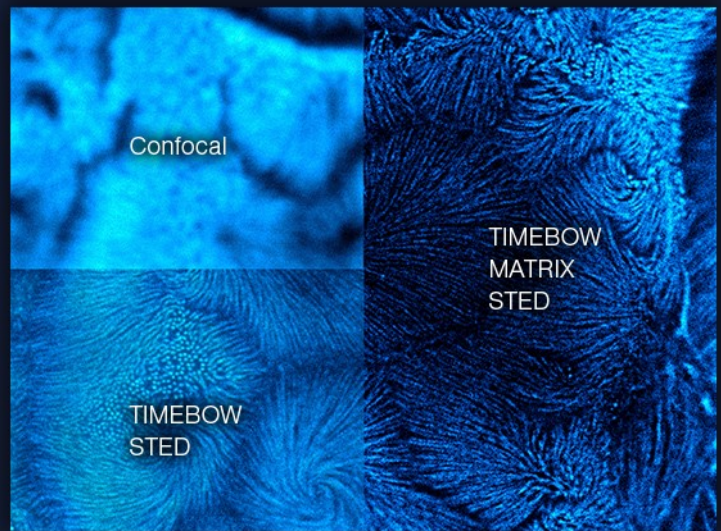
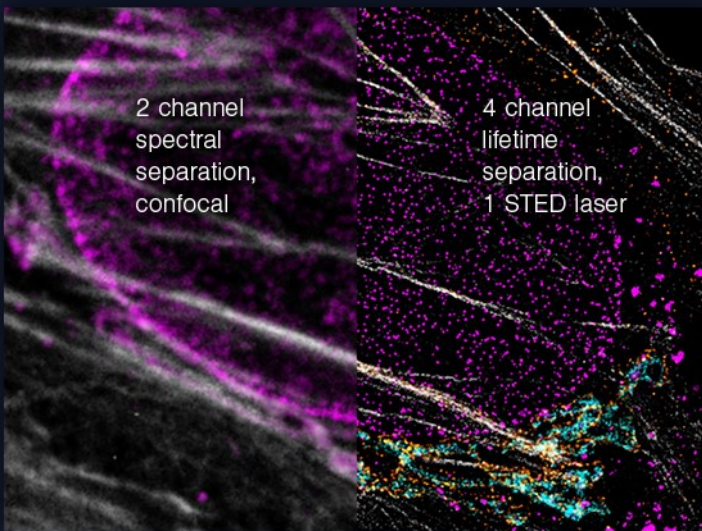
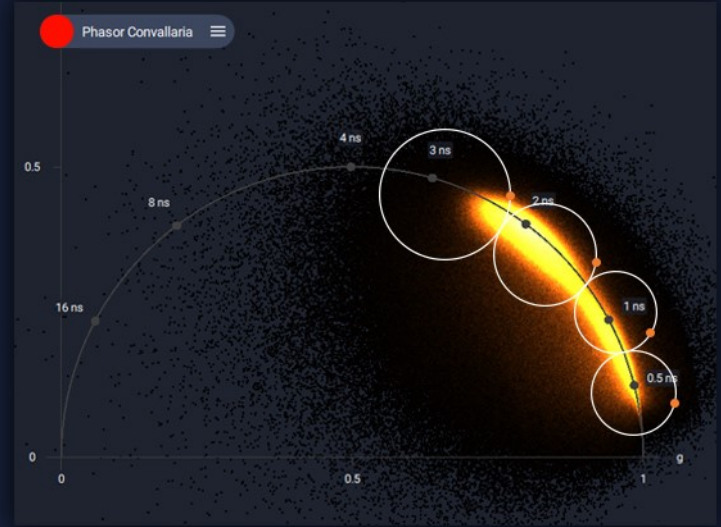
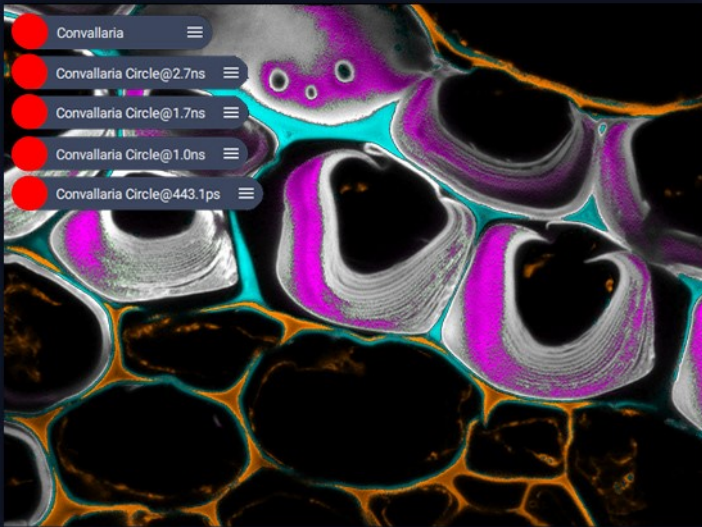
Journal of Microscopy 286(2), <https://doi.org/10.1111/jmi.13087>

Funding acknowledgement:

194812 - Enhanced Durability Predictions of Reinforced Concrete Exposed to Corrosive Environments (follow-up proposal) (SNF)
141853 - Digital Fabrication - Advanced Building Processes in Architecture (SNF)

TIMEBOW gives time a color

Lifetime separation with *TIMEBOW* is a piece of cake. Just draw circular filters on the phasor plot in the software.



Four colors with only one STED laser?
No problem, thanks to *TIMEBOW*!

Boost resolution to the max with *MATRIX* array detection coupled with *TIMEBOW* lifetime imaging, only from *abberior*!

[Learn more >](#)

abberior is all about breaking barriers. With *TIMEBOW*, we have once again succeeded. *TIMEBOW* is a reliable method for measuring fluorescence lifetime with and without super resolution. In combination with our highly sensitive APDs and the groundbreaking *MATRIX* detector, you get the best out of every aspect of the signal – as easy as 1-2-3! With *TIMEBOW*, your research shines in perfect color.

Microstructural examination of carbonated 3D-printed concrete

Asel Maria Aguilar Sanchez¹ | Timothy Wangler¹  | Matteo Stefanoni² | Ueli Angst²

¹Physical Chemistry of Building Materials, Institute for Building Materials, ETH Zurich, Zurich, Switzerland

²Durability of Engineering Materials, Institute for Building Materials, ETH Zurich, Zurich, Switzerland

Correspondence

Timothy Wangler, Physical Chemistry of Building Materials, Institute for Building Materials, ETH Zurich, Zurich, Switzerland.

Email: wangler@ifb.baug.ethz.ch

Funding information

Open Access Funding provided by Eidgenössische Technische Hochschule Zurich.

[Correction added on 14 April 2022, after first online publication: CSAL funding statement has been added.]

Abstract

The recent interest in 3D printing with concrete has generated great interest on how inhomogeneities arise and affect performance parameters, in particular strength and durability. With respect to durability, of particular interest is how 3D-printed layer interfaces can impact transport of species of interest, such as moisture, chlorides or carbon dioxide in carbonation processes. This is of particular interest considering that the primary use case of 3D-printed concrete has been as a lost formwork for a cast structural concrete, and thus it is of interest to determine the carbonation resistance. This study consists of a preliminary look at the microstructure after accelerated carbonation of a 3D-printed concrete used as a lost formwork. Preferential carbonation is observed in the layer interfaces compared to the bulk of the printed filaments, possibly related to porosity from air voids or a locally high capillary porosity corresponding to the lubrication layer.

KEYWORDS

carbonation, concrete, digital fabrication, 3D printing, lubrication layer, microstructure

1 | INTRODUCTION

Digital fabrication with cementitious materials, or digital fabrication with concrete (DFC) has emerged in recent years as a hot topic in research due to its potential to revolutionise a long-stagnant construction sector.^{1,2} Numerous benefits are hoped to be realised with the technologies, particularly increased productivity and increased sustainability of concrete components. These two benefits are expected to be derived primarily from the hallmark of the technology, which is the removal of traditional formwork: more shape freedom for more material-efficient structures enhances sustainability, and removal of form-

work labour removes a major labour cost and time burden in production of concrete components.³

The dominant DFC method employed to date has been layered extrusion^{4,5} (often called 3D concrete printing, or Contour Crafting, the brand name of its first major developer). The method consists of subsequent placement of filaments of cementitious material to eventually build up a component. The method has until now primarily been utilised to produce lost formworks, because of the inability to efficiently incorporate traditional steel reinforcement in the vertical direction.^{6–8} In fact, the most visible industrial use case has been the production of masonry structures with integrated formworks for structural columns,

This is an open access article under the terms of the [Creative Commons Attribution](https://creativecommons.org/licenses/by/4.0/) License, which permits use, distribution and reproduction in any medium, provided the original work is properly cited.

© 2022 The Authors. *Journal of Microscopy* published by John Wiley & Sons Ltd on behalf of Royal Microscopical Society

to which passive reinforcement is later added and a structural concrete cast.^{3,9–12} This method inherently produces a layered structure, and while the effect of the layer interfaces has produced most research interest related to their effect on the mechanical properties,^{13–16} recently research has started to focus on how the layer interfaces can impact durability.¹⁷ To that end, some studies have focused on moisture transport in the layer interfaces,^{18,19} and some recent studies have focused on chloride transport as well.^{20,21} Other studies have explicitly focused on analysis of the microstructure of the layer interfaces, with the air void system and the porosity being the primary focus point.^{22–26} Until now, however, only one very recent study has examined carbonation of printed concrete,²⁷ and in this study, the microstructure of the carbonated concrete was not examined. Additionally, until now, most studies have focused on unaccelerated 3D-printed mixes, which generally have high viscosities, high initial yield stresses, and low buildability rates.

In this study, we report results on the microstructure of carbonated printed concrete as examined by optical thin section and SEM-EDX. The concrete of this study is also printed through use of a set accelerator, with a low viscosity and low initial yield stress but a rapid buildability rate. Samples were produced as they would be expected to be used, that is through the use of 3D-printed concrete as a formwork for a cast concrete. Good structural engineering design would demand the placement of reinforcement bars as close to the edge of the structural element as possible (where tension is highest), but design codes also demand a concrete cover to mitigate corrosion by carbonation. Therefore, it is worth examining if printed concrete could conceivably be used as a cover layer in 3D-printed components, and our analysis of this 3D-printed sample is made with this in mind.

2 | MATERIALS AND METHODS

2.1 | Material mixes

2.1.1 | 3D-printed mix

The mix used for 3D printing has also been reported elsewhere.^{8,28} Briefly, it consists of a CEM I binder (Holcim Normo 5) with fine limestone and silica fume substitutions (15% and 8%, respectively), a superplasticizer, a viscosity modifier and sucrose to ensure the mix open time. This is added to a crushed limestone sand with max grain size of 2 mm, mixed with water at w/b of 0.39 and sand to binder ratio of 1.9, before eventually being mixed in the print nozzle with an accelerator paste consisting of cal-

cium aluminate cement (CAC) which is also retarded with sodium gluconate, at an approximate dosage of 10% OPC substitution.

2.1.2 | Cast concrete mix

The mix for the cast concrete was a standard C20/25 mix with a CEM I 42.5 N (Holcim Normo 4) at $w/c = 0.6$ and maximum grain size of 16 mm.

2.2 | Sample production and carbonation

Printed samples were produced by the 3D printing process at ETH Zurich also described in.^{8,28} They were first printed as hollow square (25 cm × 25 cm) specimens with an approximate filament width of 3.5–4 cm and a layer height of 0.5 cm, up to a total height of 25 cm. The robot moved at a speed of 200 mm/s, thus with an effective layer interval time of a few seconds. After printing, the samples were cured in ambient conditions for 10 days before the cast concrete was added within the printed formwork. The concrete was stored at ambient conditions for another 2 months before they were placed in a carbonation chamber.

The samples were carbonated in accelerated conditions in a self-made carbonation chamber made of a sealed box connected to a CO₂ gas bottle. The CO₂ level was maintained between 50% and 90% at a RH of 70% for a period of 2 months before the samples were removed.

2.3 | Sample preparation for microscopy

The produced samples were then cut and immediately had phenolphthalein and thymolphthalein applied to check for carbonation depth. Regions of interest were identified and a polished thin section was produced from layers approximately middle height (as there was no major variation observed in carbonation behaviour from top to bottom) to observe the microstructure with both optical and scanning electron microscopes.

2.4 | Microscopy

A stereo microscope Leica M 60 was used for the observation of bulk samples and a Leica DM750 P in both plane and polarised light mode was used for observing the thin section. SEM-EDX observation (BSE images) and point analyses were performed with a QUANTA 2003D and EDX system from EDAX company.

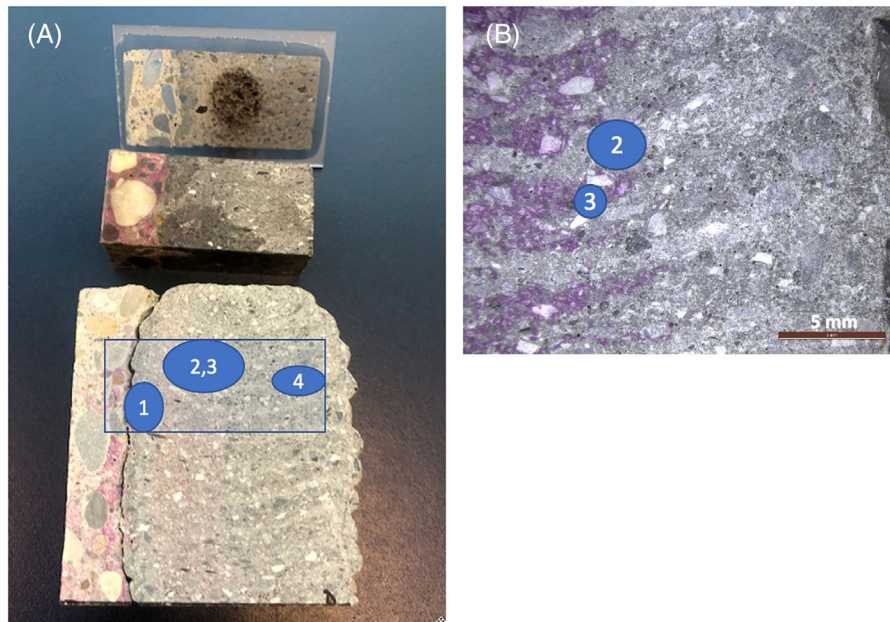


FIGURE 1 sample and corresponding thin section area (A), with zones labelled. Zone 1: close to cast–print interface. Zone 2, 3 (B): within ‘transition zone’ containing uncarbonated concrete (purple colour from phenolphthalein indicates uncarbonated zones), with 2 focused on the carbonated zone in the layer interface, and 3 focused on the uncarbonated zone. Zone 4: fully carbonated zone

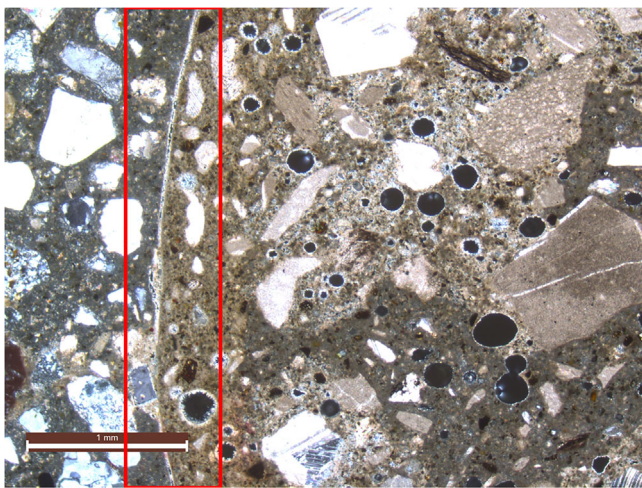


FIGURE 2 Cross polarized micrograph of Zone 1 (cast–print interface, cast concrete on left). Carbonation front observed (red box) and precipitation of calcite crystals in air voids and interfacial porosity

3 | RESULTS

Figure 1 shows the sample from which the thin section was taken, with zones of interest labelled. It can be seen that significant carbonation has taken place over the depth of the printed concrete, and that this occurs inhomogeneously, apparently corresponding to a higher degree of carbonation in the layer interfaces than in the bulk of the interlayers. There exist four interesting zones

in the printed sample. First, there is a zone next to the cast concrete that is carbonated next to an uncarbonated zone (Zone 1), then there is a ‘transition zone’ consisting of carbonated concrete in the interlayer zone and uncarbonated concrete in within the bulk of the layer (Zones 2 and 3, respectively) and then there is a fully carbonated zone extending from the exposure surface to approximately 2–3 cm into the printed concrete (Zone 4).

In Figure 2, one sees an optical thin section of the cast–print interface. One can clearly see here a uniform and very dense carbonation front extending to approximately 0.5 mm from the cast–print interface, and the precipitation of calcite crystals (confirmed by SEM-EDX) in air voids and within the interface. It should also be noted that in SEM-BSE, it was observed that the degree of hydration in this zone was quite advanced, with almost no anhydrous cement observed. It was also observed that carbonation was not homogeneous, with very dense areas and other areas of high porosity. General microcracking was observed everywhere within the printed concrete as well.

Figure 3 focuses on Zones 2 and 3, where a cross-polarised optical micrograph shows a clearly densified region of carbonation approximately 1 mm in thickness at the layer interface. SEM-BSE images focused on each of the zones show a difference in hydration degree, with the bulk layer region (Zone 3) tending to show lower degree of hydration, with larger unhydrated particles. In the carbonated region, similar to Zone 1, the carbonation was not homogeneous. Microcracking was also observed everywhere.

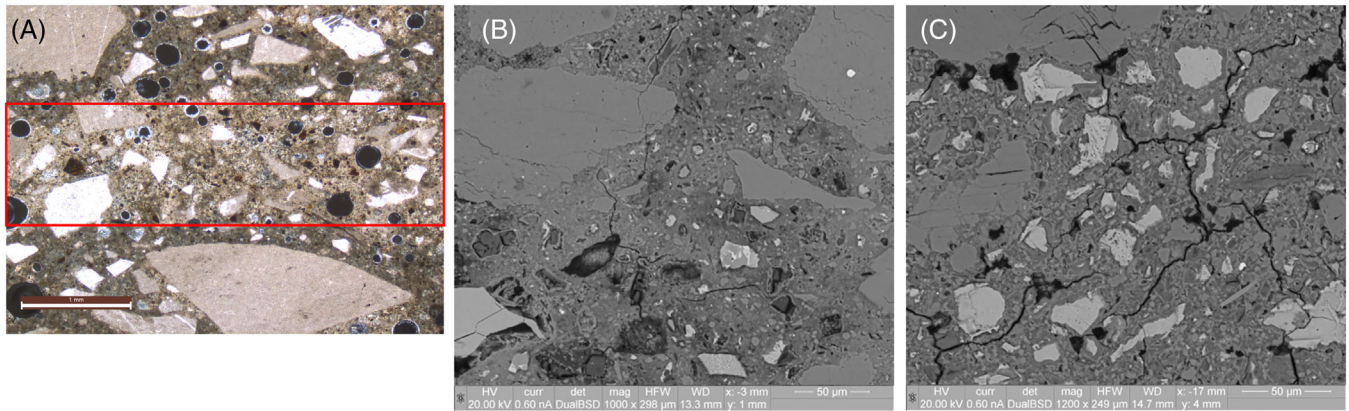


FIGURE 3 cross-polarized optical micrograph of Zones 2 and 3 (A) and SEM-BSE micrograph of Zone 2 (B) and Zone 3 (C). Clearly carbonated region seen approximately 1 mm in thickness (in red) at the printed layer interface. Larger unhydrated cement particles apparent in Zone 3 compared to Zone 2

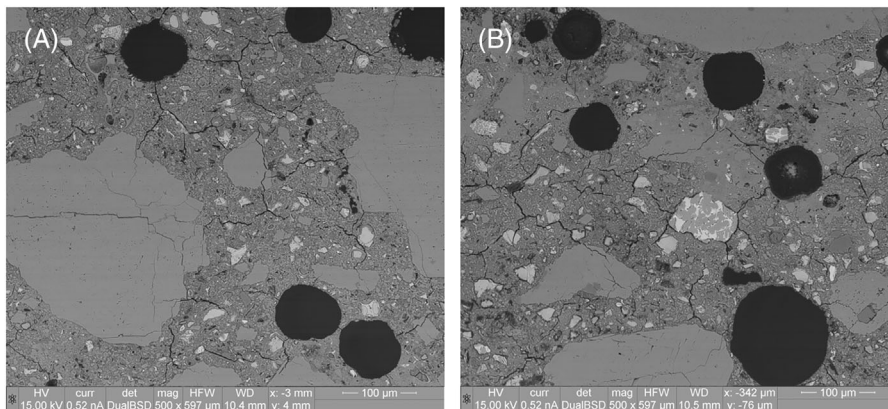


FIGURE 4 SEM-BSE images of fully carbonated region of Zone 4, with interfacial zone (A) and bulk zone (B). Higher degree of hydration observed in interfacial zone compared to bulk

Figure 4 shows SEM-BSE micrographs of Zone 4, focusing on both the interfacial and the bulk layer zones as well. Similar to Figure 3, larger unhydrated cement particles with more poorly developed hydration rims are seen in the bulk region compared to the layer interface region. The amount of carbonation observed is also still higher in the layer interface region compared to the bulk region, and again microcracking is observed everywhere. Finally, it was observed that the air void sizes tended to be larger at the layer interface region.

4 | DISCUSSION

At the cast–print interface, one can observe a separation between the printed and cast layers, which could be due to drying shrinkage differences between the two materials and their different production times. The uniform carbonation depth of 0.5 mm in the printed concrete is likely

due to the 10 days delay between the printing and the casting, however, because no corresponding carbonation depth was observed in the cast concrete. It is also worth noting that the highly advanced degree of hydration in this zone could be due to sorption of water from the cast concrete. Overall, examination of this region highlights the importance of understanding the relationship between printed formworks and cast concrete in terms of the overall process and performance.

In the ‘transition zone’ (Zones 2 and 3), it is quite apparent that carbonation is occurring nonuniformly within the printed concrete, and that it is occurring with greater speed within the layer interfaces, indicative of a difference in the diffusivity between the layer interfaces and the bulk. This higher carbonation speed in the layer interfaces contributes to faster carbonation in the bulk of the print filament as well, essentially by allowing carbonation from the top and bottom of the filament and effectively reducing the diffusion length.

It is interesting to note that the thickness of the carbonation layer at the layer interface is approximately 1 mm. It is well known that a ‘lubrication layer’ forms during pumping of concrete, in which a paste rich zone forms at the wall of the pipe,^{29,30} and it has been noted that this lubrication layer could also be present after extrusion of concrete, and thus responsible at least in part for heterogeneity across the filament cross section.³¹ The size of this lubrication layer has been measured through various techniques and estimated to be on the order of 1–5 mm.³² This increase in paste content, however, is likely not responsible for the enhanced transport in the layer interfaces, because it has been demonstrated that paste volume does not play a large role in the carbonation depth.³³ It is much more likely that there is another factor at play, and the most likely reasons are increased porosity from air voids, or increased capillary porosity.

As noted earlier, most studies to date have focused on presence of defects and air voids in the interlayer, with a primary focus on their effect on the strength. Numerous X-ray micro computerised tomography studies have detailed their presence and extent with respect to processing parameters such as printhead speed, pressure, and height, layer interval time, and ambient conditions with respect to moisture,^{23–27} with only one directly linking the measurements to durability performance metrics.²⁷ However, the rheology of each of these systems stands in stark contrast to the rheology of the 3D printing system used in this study. The rheology in this study is much more fluid, practically self-compacting upon exit from the nozzle (yield stress ~ 500 Pa, with a correspondingly low viscosity³⁴), and thus fluid enough to allow entrapped air to escape. While it was observed that the air voids were slightly larger in the layer interfaces, other possibilities for faster carbonation should be explored, including the possibility of increased capillary porosity.

Capillary porosity is strongly influenced by the w/c ratio. The same physical principle that leads to a depletion of aggregate next to the wall will also lead to a depletion of binder particles, which would lead to an effective increase in the w/c ratio within a certain range of the layer interface. This moisture content is enhanced by pressurised bleeding, noted by Sanjayan et al.¹⁵ and Kosson et al.³⁵ A locally higher w/c ratio would manifest itself in a higher degree of hydration, which was observed in this sample, across the width of the layer interface. This is corroborated by Van Der Putten et al.,²⁶ who also found a lower proportion of unhydrated cement particles at the layer interface. This phenomenon could be the source of the higher degree of hydration at the cast–print interface, as the lubrication layer is formed around the entire extrusion filament. In any case, a locally high w/c at the layer interface would lead to a higher capillary porosity and thus enhanced transport.

The dense carbonation layer at the layer interface could also be indirect evidence of this locally high capillary porosity. One would expect that carbonation products would form generally where there is a high amount of portlandite, such as in the traditional interfacial transition zone (ITZ). For example, Shen et al. demonstrated that carbonation products formed significantly in the ITZ.³⁶ The layer interface could also be considered similar to an ITZ, and a locally high w/c and concomitantly higher capillary porosity would allow portlandite to precipitate there preferentially, thus also to carbonate there preferentially.

A final discussion point could be made regarding the high degree of microcracking observed. While this could easily be related to sample preparation, it could also bear some relation to material, processing, and shrinkage. The printed material is essentially a binary OPC-CAC system, relying on ettringite formation to develop rapid buildability strength.³⁷ Inhomogeneities in mixing and especially across the filament cross section could lead to differential displacements due to differential shrinkages from drying, or from carbonation of the portlandite or ettringite. The microcracking, if it comes from one of these processes, could also act as an enhancer of CO_2 transport.

5 | CONCLUSIONS AND OUTLOOK

The primary conclusions and recommendations that can be drawn from this preliminary look at the microstructure of carbonated 3D-printed concrete are the following:


- The 3D-printed concrete of this study showed nonuniform carbonation due to the presence of the layer interfaces, with the layer interfaces showing faster carbonation. This can be from enhanced transport due to either increased air content or capillary porosity in the layer interface. The implications for this require further study, as this would negatively impact the possibility of using a printed formwork as a cover layer.
- The interface of a structural concrete cast into a 3D-printed formwork (‘cast–print’ interface) requires attention in future studies, especially as this represents the predominant use case of this technology.
- A more complete study is needed regarding the generation and evolution of microstructural heterogeneities in 3D-printed concrete with respect to carbonation, in particular with respect to the capillary porosity at the layer interfaces.

ACKNOWLEDGEMENTS

The authors would like to thank Ana Anton for her support in the sample production, as well as Prof. Robert J. Flatt for useful discussions and insights. The authors

acknowledge the Swiss National Science Foundation for funding in support of this research (project PP00P2_194812 / 1, as well as the NCCR Digital Fabrication, Agreement #51NF40-141853).

ORCID

Timothy Wangler  <https://orcid.org/0000-0003-2839-6433>

REFERENCES

- Bos, F., Wolfs, R., Ahmed, Z., & Salet, T. (2016). Additive manufacturing of concrete in construction: Potentials and challenges of 3D concrete printing. *Virtual and Physical Prototyping*, *11*, 209–225.
- Wangler, T., Roussel, N., Bos, F. P., Salet, T.A.M., & Flatt, R.J. (2019). Digital concrete: A review. *Cement and Concrete Research*, *123*, 105780.
- Kreiger, E. L., Kreiger, M. A., & Case, M. P. (2019). Development of the construction processes for reinforced additively constructed concrete. *Additive Manufacturing*, *28*, 39–49.
- Buswell, R. A., De Silva, W. R. L., & Jones, S. Z. (2018). 3D printing using concrete extrusion: A roadmap for research. *Cement and Concrete Research*, *112*, 37–49.
- Khoshnevis, B. (2004). Automated construction by contour crafting—Related robotics and information technologies. *Automation in Construction*, *13*, 5–19.
- Gaudillière, N., Duballet, R., Bouyssou, C., Mallet, A., Roux, P., & Zakeri, M. (2019). Chapter 3 – Building applications using lost formworks obtained through large-scale additive manufacturing of ultra-high-performance concrete. In J.G. Sanjayan, A. Nazari, & B. Nematollahi (Eds.), *3D concrete printing technology* (pp. 37–58). Butterworth-Heinemann.
- Asprone, D., Menna, C., Bos, F. P., Salet, T.A., Mata-Falcón, J., & Kaufmann, W. (2018). Rethinking reinforcement for digital fabrication with concrete. *Cement and Concrete Research*, *112*, 111–121.
- Anton, A., Reiter, L., Wangler, T., Frangez, V., Flatt, R. J., & Dillenburger, B. (2021). A 3D concrete printing prefabrication platform for bespoke columns. *Automation in Construction*, *122*, 103467.
- AS MASONRY. Apis Cor Accessed March 8, (2020). <https://www.apis-cor.com/as-masonry>.
- PERI. (2020). November 17, 2020 Accessed April 26, 2021. <https://www.peri.com/en/business-segments/3d-construction-printing.html>.
- Wangler, T. (2020). Digital fabrication in concrete construction. In R. Mangabhai (Ed.), *The Institute of Concrete Technology Yearbook: 2020–2021* (pp. 61–69). Institute for Concrete Technology.
- Zhu, B., Nematollahi, B., Pan, J., Zhang, Y., Zhou, Z., & Zhang, Y. (2021). 3D concrete printing of permanent formwork for concrete column construction. *Cement and Concrete Composites*, *121*, 104039.
- Wolfs, R. J. M., Bos, F. P., & Salet, T. A. M. (2019). Hardened properties of 3D printed concrete: The influence of process parameters on interlayer adhesion. *Cement and Concrete Research*, *119*, 132–140.
- Nerella, V. N., Hempel, S., & Mechtcherine, V. (2018). Effects of layer-interface properties on mechanical performance of concrete elements produced by extrusion-based 3D-printing. *Construction and Building Materials*, *205*, 586–601.
- Sanjayan, J. G., Nematollahi, B., Xia, M., & Marchment, T. (2018). Effect of surface moisture on inter-layer strength of 3D printed concrete. *Construction and Building Materials*, *172*, 468–475.
- Keita, E., Bessaies-Bey, H., Zuo, W., Belin, P., & Roussel, N. Weak bond strength between successive layers in extrusion-based additive manufacturing: Measurement and physical origin. *Cement and Concrete Research*, *123*, 105787.
- Kruger, J., & van Zijl, G. (2021). A compendious review on lack-of-fusion in digital concrete fabrication. *Additive Manufacturing*, *37*, 101654.
- Schröfl, C., Nerella, V. N., & Mechtcherine, V. (2019). Capillary water intake by 3D-printed concrete visualised and quantified by neutron radiography. In T. Wangler & R.J. Flatt (Eds.), *First RILEM International Conference on Concrete and Digital Fabrication – Digital Concrete 2018* (pp. 217–224). Springer International Publishing.
- Van Der Putten, J., Azima, M., Van den Heede, P., Mullem, T. V., Snoeck, D., Carminati, C., Hovind, J., Trtk, P., De Schutter, G., & Tittelboom, K. V. (2020). Neutron radiography to study the water ingress via the interlayer of 3D printed cementitious materials for continuous layering. *Construction and Building Materials*, *258*, 119587.
- Van Der Putten, J., De Volder, M., Van den Heede, P., De Schutter, G., & Tittelboom, K. V. (2020). 3D printing of concrete: The influence on chloride penetration. In *Second RILEM International Conference on Concrete and Digital Fabrication* (pp. 500–507). Springer International Publishing.
- Bran-Anleu, P., Wangler, T., Nerella, V. N., Mechtcherine, V., Trtk, P., & Flatt, R. J. Using micro-XRF to characterize chloride ingress through cold joints in 3D-printed concrete. (submitted)
- Cicione, A., Kruger, J., Walls, R. S., & Zijl, G. V. (2020). An experimental study of the behavior of 3D printed concrete at elevated temperatures. *Fire Safety Journal*, *120*, 103075.
- Chen, Y., Çopuroğlu, O., Rodriguez, C. R., de Mendonca Filho, F. F., & Schlangen, E. (2021). Characterization of air-void systems in 3D printed cementitious materials using optical image scanning and X-ray computed tomography. *Materials Characterization*, *173*, 110948.
- Kruger, J., du Plessis, A., & van Zijl, G. (2021). An investigation into the porosity of extrusion-based 3D printed concrete. *Additive Manufacturing*, *37*, 101740.
- Geng, Z., She, W., Zuo, W., Lyu, K., & Pan, H. (2020). Layer-interface properties in 3D printed concrete: Dual hierarchical structure and micromechanical characterization. *Cement and Concrete Research*, *138*, 106220.
- Van Der Putten, J., Deprez, M., Cnudde, V., De Schutter, G., & Tittelboom, K.V. (2019). Microstructural characterization of 3D printed cementitious materials. *Materials*, *12*.
- Zhang, Y., Zhang, Y., Yang, L., Liu, G., Chen, Y., Yu, S., & Du, H. (2021). Hardened properties and durability of large-scale 3D printed cement-based materials. *Materials and Structures*, *54*, 45.
- Anton, A., Bedarf, P., Yoo, A., Dillenburger, B., Reiter, L., Wangler, T.P., Flatt, R. J., Burry, J., Sabin, J., Sheil, B., & Skavara, M. (2020). Concrete Choreography: Prefabrication of 3D-printed columns. In *Fabricate 2020: Making resilient architecture* (pp. 286–293). UCL Press.

29. De Schutter, G., & Feys, D. (2016). Pumping of fresh concrete: Insights and challenges. *RILEM Technical Letters*, 1, 76–80.
30. Feys, D. (2012). 13 – Understanding the pumping of conventional vibrated and self-compacting concrete. In N. Roussel (Ed.), *Understanding the rheology of concrete* (pp. 331–353). Woodhead Publishing.
31. Mechtcherine, V., Bos, F. P., Perrot, A., da Silva, W.R. L., Fataei, S., Wolf, R.J.M., Sonebi, M., & Roussel, N. (2020). Extrusion-based additive manufacturing with cement-based materials – Production steps, processes, and their underlying physics: A review. *Cement and Concrete Research*, 132, 106037.
32. Choi, M., Roussel, N., Kim, Y., & Kim, J.-K. (2013). Lubrication layer properties during concrete pumping. *Cement and Concrete Research*, 45, 69–78.
33. Hermida, G., Moranville, M., & Flatt, R. J. (2009). The role of paste volume on performance of concrete. In P.G.T.C.H. Malhotra (Ed.), *Proceedings Tenth ACI International Conference on Recent Advances in Concrete Technology and Sustainability Issues* (pp. 201–214). American Concrete Institute.
34. Reiter, L., Anton, A.-M., Wangler, T., Dillenburger, B., & Flatt, R. J. Layered extrusion - processing and set on demand. (in process).
35. Kosson, M., Brown, L., & Sanchez, F. (2020). Early-age performance of 3D printed carbon nanofiber and carbon microfiber cement composites. *Transportation Research Record*, 2674, 10–20.
36. Qizhen, S., Ganghua, P., & Huagang, Z. (2017). Effect of interfacial transition zone on the carbonation of cement-based materials. *Journal of Materials in Civil Engineering*, 29, 04017020.
37. Reiter, L., Wangler, T., Anton, A., & Flatt, R. J. (2020). Setting on demand for digital concrete – Principles, measurements, chemistry, validation. *Cement and Concrete Research*, 132, 106047.

How to cite this article: Sanchez, A.M.A., Wangler, T., Stefanoni, M., & Angst, U. (2022). Microstructural examination of carbonated 3D – printed concrete. *Journal of Microscopy*, 286, 141–147. <https://doi.org/10.1111/jmi.13087>